JOURNAL OF COMPUTATIONAL PHYSICS 64, 389–415 (1986)

# A Space-Marching Method for Viscous Incompressible Internal Flows

M. POUAGARE AND B. LAKSHMINARAYANA

*Department of Aerospace Engineering, The Pennsylvania State University, 153 Hammond Building, University Park, Pennsylvania 16802*

Received November 19, 1984; revised September 20, 1985

This paper deals with the development of a space-marching method for steady incompressible flows. The method solves the continuity and the momentum equations as a coupled system at each streamwise station. The character of the system of equations is changed from elliptic to hyperbolic/parabolic in order to enable the equations to be marched in space. The present method has two main advantages compared to the existing parabolic or space-marching methods for an incompressible flow: (i) It avoids the solution of Poisson equations, and (ii) conserves the mass flow without employing any iterative procedure. The present method can capture strong secondary velocities and strong transverse pressure gradients. Predictions of the flow through straight and strongly curved ducts are in good agreement with the analytical and the experimental results. 

## INTRODUCTION

In many flows of practical application, a dominant flow direction can be identified, such as the flow through ducts and turbomachinery blade rows. These flows can be predicted by marching, along the dominant flow direction, an approximate form of the steady Navier–Stokes equations.

The major difficulty in solving the steady Navier–Stokes equations for subsonic flows as a parabolic system of equations is that these equations are actually elliptic in nature. In subsonic flows, the terms that prevent the equations from being parabolic in the streamwise direction are the streamwise pressure gradient term and the streamwise viscous diffusion term. The latter is, in general. a small term and is neglected with no loss of accuracy. The streamwise pressure gradient term is very important, and, thus, it is always retained. Different researchers use different methods to treat the streamwise pressure gradient.

Patankar and Spalding [1] introduced a bulk streamwise pressure gradient correction and assumed uniform over the cross flow direction, in order to ensure conservation of global mass flow. To ensure local conservation of mass flow, they solved a pressure equation derived from the continuity equation. Briley [2] and Ghia, Ghia, and Studerus [3] used a similar procedure as Patankar and Spalding as far as the streamwise pressure gradient is concerned. Their scheme requires the



0021-9991/86 $3.00



581/64/2-8

solution of two Poisson equations in order to ensure local mass conservation and to estimate the transverse pressure gradients. Many other researchers (e.g., see [4, 5]) have developed methods similar to the above-mentioned.

Briley and McDonald [6] follow a somewhat different approach. They split the velocity into four parts: (i) potential primary velocity (assumed known), (ii) potential secondary velocity, (iii) solenoidal secondary velocity, and (iv) viscous streamwise velocity correction. They recast the equations of motion in order to obtain equations for each of the velocity parts and the pressure. Their method requires a priori knowledge of the potential flow.

All these methods, classified as parabolic methods, have been used primarily for the prediction of flows in channels and ducts. Their major difficulty is in satisfying the mass conservation through the solution of some kind of Poisson equation for the pressure. Another shortcoming is that they solve the equations as an uncoupled system, and they rely on iterative procedures to couple them. The uncoupling of the equations is imperative because of the different types of equations employed. Most commonly, the equation that forces the uncoupled solution of the system of equations is the Poisson equation for the pressure. All of these methods are designed and used for subsonic flow computations.

The solution of supersonic flows with methods that march the equations along the dominant flow direction is "easier" than the solution of subsonic flows. In supersonic flows, the Navier–Stokes equations are hyperbolic in the streamwise direction when the streamwise viscous diffusion terms are dropped. This is because the streamwise pressure gradient term does not introduce ellipticity in a supersonic flow. Therefore, no special treatment is required for this term. However, in supersonic flows, there is usually a small subsonic region in the flow field very near the solid surfaces inside the boundary layer. Since the flow is subsonic in this region, the streamwise pressure gradient term introduces ellipticity there. This is easily overcome by treating the streamwise pressure gradient term in the subsonic region as a known source term derived from the supersonic part of the flow.

Many parabolic methods have been developed for supersonic flows. Some of the references in this area are the following: Lin and Rubin [7], McDonald and Briley [8], Vigneron, Rakich, and Tannehill [9], Lubard and Helliwell [10], and Schiff and Steger [11]. Usually, the methods developed for supersonic flows are referred to as space-marching methods. This is because these methods resemble the time-marching methods. The space-marching methods for supersonic flows solve the governing equations (continuity, three-momentum, and energy) in steady form as a coupled system by marching in the streamwise direction. Therefore, they do not have any problem in conserving mass, and they do not need to employ any special equation for the pressure. These methods are economical, elegant, straightforward, and easy to comprehend, code, and debug. Only recently did Govindan [12] recognize the advantages of applying space-marching methods developed for supersonic flows to subsonic flows.

Govindan [12] adapted Schiff and Steger's space-marching method to subsonic internal flows. The major difference between the application of this space-marching

method in subsonic flows and the application of the same method in supersonic flows is the following: in subsonic flows, the streamwise pressure gradient is treated everywhere as a known source term, while, in supersonic flows, the streamwise pressure term is treated as a known source term only in the small subsonic region near solid walls.

In subsonic flows, the treatment of the streamwise pressure gradient term as a known source term is what changes the character of the equations from ellitic to parabolic, and enables the marching of the equations in space.

Some difficulties were encountered in using Govindan's method in incompressible flows, in that the method is sensitive to the specified streamwise pressure gradient. This motivated the authors to develop a space-marching method specifically for incompressible flows. The present paper deals with the development of a method for incompressible flows, employing ideas used in space-marching methods for supersonic flows.

## Present Method

To illustrate the present method, the 2-dimensional non-dimensionalized incompressible equations are used. The streamwise viscous diffusion terms are neglected, and the equations are written in a Cartesian coordinate system $(x, y)$ with the $x$ axis aligned with the streamwise direction:

$$\frac{\partial A(q)}{\partial x} + \frac{\partial B(q)}{\partial y} = \frac{1}{R_e}\frac{\partial^2 D(q)}{\partial y^2} \tag{1}$$

where

$$A = \begin{bmatrix} u \\ u^2 + p \\ uv \end{bmatrix}; \qquad B = \begin{bmatrix} v \\ uv \\ v^2 + p \end{bmatrix}; \qquad D = \begin{bmatrix} 0 \\ u \\ v \end{bmatrix}$$

where $p$ is the static pressure, $u$ and $v$ are velocity components in $x$ and $y$ directions respectively, $R_e$ is the Reynolds number, and $q$ is the vector of unknowns, given by

$$q = [p, u, v]^T.$$

As expected, the eigenvalue analysis of the system of equations (1) showed that, in order to be able to solve this set of equations by marching in the streamwise direction $x$, the pressure $p$ in the streamwise flux vector $A$ must be treated as a known source term. Therefore, $A$ is replaced by $A_s$ and $A_p$, given by

$$A_s = \begin{bmatrix} u \\ u^2 \\ uv \end{bmatrix}; \qquad A_p = \begin{bmatrix} 0 \\ p_{as} \\ 0 \end{bmatrix} \tag{2}$$

where $p_{as}$ can be estimated from an inviscid solution of the flow field and $A_p$ is treated as a source term.

A necessary condition for marching any set of equations is that the Jacobian matrix of the streamwise flux vector be non-singular. Unfortunately, the Jacobian matrix of $A_s$, given by

$$A_{sJ} = \begin{bmatrix} 0 & 1 & 0 \\ 0 & 2u & 0 \\ 0 & v & u \end{bmatrix} \tag{3}$$

is singular. When using the compressible set of equations, this problem does not arise because of the presence of the energy equation in the set of equations.

Therefore, at this point, the solution by marching technique seems impossible. This is because, if $p$ is included in the streamwise flux vector, the set of equations is elliptic and cannot be space marched, and, if it is removed, the Jacobian matrix of the streamwise flux vector becomes singular.

However, a careful examination of the eigenvalue of the system of Eq. (1) provided the clue for overcoming the above-mentioned problems.

Before proceeding to the eigenvalue analysis, in order to keep track of the pressure term in the streamwise flux vector $A$, a coefficient $\sigma$ ($\sigma = 1$) multiplying $p$ is introduced in vector $A$. Thus, vector $A$ is now given by the expression:

$$A = \begin{bmatrix} u \\ u^2 + \sigma p \\ uv \end{bmatrix} \tag{4}$$

In order to perform the eigenvalue analysis, a linearized frozen coefficient form of Eq. (1) is considered:

$$A_J \frac{\partial q}{\partial x} + B_J \frac{\partial q}{\partial y} = \frac{1}{R_e} D_J \frac{\partial^2 q}{\partial y^2} \tag{5}$$

where $A_J$, $B_J$, and $D_J$ are the Jacobian matrices of $A$, $B$, and $D$, respectively. $A_J$, $B_J$, and $D_J$ are given by the following expressions:

$$A_J = \begin{bmatrix} 0 & 1 & 0 \\ \sigma(=1) & 2u & 0 \\ 0 & v & u \end{bmatrix}; \quad B_J = \begin{bmatrix} 0 & 0 & 1 \\ 0 & v & u \\ 1 & 0 & 2v \end{bmatrix}; \quad D_J = \begin{bmatrix} 0 & 0 & 0 \\ 0 & 1 & 0 \\ 0 & 0 & 1 \end{bmatrix} \tag{6}$$

Equation (5) is rewritten as follows:

$$\frac{\partial q}{\partial x} + (A_J^{-1} B_J) \frac{\partial q}{\partial y} = \frac{1}{R_e} (A_J^{-1} D_J) \frac{\partial^2 q}{\partial y^2}. \tag{7}$$

For stable streamwise marching of Eq. (7), the eigenvalues of $A_J^{-1}B_J$ must be real, and the eigenvalues of $A_J^{-1}D_J$ must be non-negative (see [9]). The former condition is required in the inviscid region of the flow for the equations to be hyperbolic, and the latter condition is required in the viscous region of the flow for positive viscosity to cause damping in the marching direction.

The characteristic equation and the eigenvalues of $A_J^{-1}D_J$ are given by the following expressions:

$$\lambda^2\left(\frac{1}{u}-\lambda\right)=0 \tag{8}$$

$$\lambda_{1,2}=0; \qquad \lambda_3=\frac{1}{u}. \tag{9}$$

Therefore, $A_J^{-1}D_J$ has non-negative eigenvalues as long as $u>0$ (i.e., non-separated flow). This restriction is common to all parabolic or space-marching methods.

The characteristic equation and the eigenvalues of $A_J^{-1}B_J$ are given by the following expressions:

$$\lambda^3-\left(\frac{v}{u}\right)\lambda^2+\frac{\lambda}{\sigma}-\left(\frac{v}{u}\right)\frac{1}{\sigma}=0 \tag{10}$$

$$\lambda_1=\frac{i}{\sqrt{\sigma}}; \qquad \lambda_{2,3}=-\frac{1}{2}\left(\frac{i}{\sqrt{\sigma}}-\frac{v}{u}\right)\pm\frac{1}{2}\sqrt{(i/\sqrt{\sigma}-v/u)^2+4iv/\sqrt{\sigma}u}. \tag{11}$$

The eigenvalues of $A_J^{-1}B_J$ are imaginary, and, thus, Eq. (1) cannot be solved by space marching in the streamwise direction.

A careful look at Eq. (11) reveals that the imaginary unit $i$ always appears together with the square root of $\sigma$. If $\sigma$ is taken to be equal to any negative number, the eigenvalues of $A_J^{-1}B_J$ become real. Setting $\sigma=-|\sigma|$, Eqs. (10) and (11) take the following forms:

$$\lambda^3-\left(\frac{v}{u}\right)\lambda^2-\frac{\lambda}{|\sigma|}+\left(\frac{v}{u}\right)\frac{1}{|\sigma|}=0;$$

$$\lambda_1=\frac{1}{|\sigma|};$$

$$\lambda_{2,3}=-\frac{1}{2}\left(\frac{1}{\sqrt{|\sigma|}}-\frac{v}{u}\right)\pm\frac{1}{2}\sqrt{(1/\sqrt{|\sigma|}-v/u)^2+4v/\sqrt{|\sigma|}u}$$

or

$$\lambda_{1,2}=\pm\frac{1}{\sqrt{|\sigma|}}; \qquad \lambda_3=\frac{v}{u}. \tag{12}$$

Therefore, all the eigenvalues of $A_J^{-1}B_J$ are now real. This was achieved by setting $\sigma = -|\sigma|$, where $\sigma$ is any real number. Based on this observation, $A$ is rewritten as follows:

$$A = \begin{bmatrix} u \\ u^2 - |\sigma|\, p + |\sigma|\, p + p \\ uv \end{bmatrix}. \tag{13}$$

$A$ is split into $A_\sigma$ and $A_p$ as follows:

$$A_\sigma = \begin{bmatrix} u \\ u^2 - |\sigma|\, p \\ uv \end{bmatrix}; \qquad A_p = \begin{bmatrix} 0 \\ |\sigma|\, p + p \\ 0 \end{bmatrix}. \tag{14}$$

With the expressions in Eq. (14), Eq. (1) takes the form

$$\frac{\partial(A_\sigma(q) + A_p(q))}{\partial x} + \frac{\partial B(q)}{\partial y} = \frac{1}{R_e}\frac{\partial^2 D(q)}{\partial y^2}. \tag{15}$$

Equation (15) is, of course, identical to Eq. (1). Up to this point, we have done nothing more than simply adding and subtracting the term $|\sigma|\, p$ in the $x$-momentum equation. However, if $A_p$ is treated as a known source term and $A_\sigma$ is considered to be the new streamwise flux vector, Eq. (15) takes the following form:

$$\frac{\partial A_\sigma(q)}{\partial x} + \frac{\partial B(q)}{\partial y} = \frac{1}{R_e}\frac{\partial^2 D(q)}{\partial y^2} + S, \tag{16}$$

where $S = -\partial A_p/\partial x$. Equation (16) can be solved by space marching in the $x$ direction, since the Jacobian of $A_\sigma$ is non-singular, $A_{\sigma J}^{-1}B_J$ has real eigenvalues, and $A_{\sigma J}^{-1}D_J$ has non-negative eigenvalues (as long as $u > 0$). $S$ does not affect the character of the eigenvalues as long as it is evaluated from known values of $p$, either assumed or calculated at previous streamwise stations. In other words, as long as $S$ does not depend on $p^{n+1}$, it does not affect the eigenvalues; $n+1$ is the station at which the solution is sought. The treatment of pressure terms as known source terms in order to change the character of the equations from elliptic to hyperbolic/parabolic and enable the marching of the equations in space has been common practice in parabolic and space-marching methods (e.g., see [1–5, 7, 9–13]).

*The Numerical Algorithm*

Equation (16) is finite differenced according to the Euler implicit scheme:

$$\frac{(A_\sigma)^{n+1} - (A_\sigma)^n}{\Delta x} = \left[ -\frac{\partial B}{\partial y} + \frac{1}{R_e}\frac{\partial^2 D}{\partial y^2} \right]^{n+1} + S \tag{17}$$

where $n+1$ is the streamwise station at which the solution is sought, and $n$ is the

station at which the solution is known; $\Delta x$ is the step size in the streamwise direction.

In the discussion that follows, $S$ is considered to be a source term and is left without an index. A detailed discussion on the evaluation of $S$ follows in a later section.

Equation (17) is linearized by expanding the flux vectors in a Taylor series about the level $n$:

$$\begin{aligned} A_\sigma^{n+1} &= A_\sigma^n + \left(\frac{\partial A_\sigma}{\partial q}\right)^n \Delta q^n \\ B^{n+1} &= B^n + \left(\frac{\partial B}{\partial q}\right)^n \Delta q^n \\ D^{n+1} &= D^n + \left(\frac{\partial D}{\partial q}\right)^n \Delta q^n \end{aligned} \tag{18}$$

where $\partial(\cdot)/\partial q$ is the Jacobian of $(\cdot)$, and $\Delta q^n$ is given by the expression:

$$\Delta q^n = q^{n+1} - q^n. \tag{19}$$

The use of Eq. (18) in Eq. (17) results in the following linearized equation:

$$\begin{aligned} &\left[\left(\frac{\partial A_\sigma}{\partial q}\right)^n - \Delta x\left[\frac{\partial}{\partial y}\left(\left(\frac{\partial B}{\partial q}\right)^n \cdot\right) + \frac{1}{R_e}\frac{\partial^2}{\partial y^2}\left(\left(\frac{\partial D}{\partial q}\right)^n \cdot\right)\right]\right]\Delta q^n \\ &\quad = \left[-\frac{\partial B}{\partial y} + \frac{1}{R_e}\frac{\partial^2 D}{\partial y^2}\right]^n + S. \end{aligned} \tag{20}$$

The derivatives in the $y$ direction are central-differenced. For example,

$$\begin{aligned} \frac{\partial B}{\partial y} &= \frac{B_{j+1} - B_{j-1}}{2\Delta y} \\ \frac{\partial^2 D}{\partial y^2} &= \frac{D_{j+1} - 2D_j + D_{j-1}}{\Delta y^2} \end{aligned} \tag{21}$$

where $\Delta y$ and $j$ are the step size and index, respectively, in the $y$ direction.

Equation (20) can be solved efficiently at each streamwise station through the inversion of a block tridiagonal matrix with $3 \times 3$ blocks. Once $\Delta q^n$ is found, the vector of unknowns at the $n+1$ station can be found through Eq. (19).

*Evaluation of S*

The source term $S$ is made up of two terms:

$$S = \left[0,\ -|\sigma|\frac{\partial p}{\partial x} - \frac{\partial p}{\partial x},\ 0\right]^T \tag{22}$$

Term 2 is the original pressure term that introduces the inviscid elliptic information to the solution. Therefore, term 2 is evaluated from an assumed inviscid pressure field $p_{as}$

$$-\frac{\partial p}{\partial x} = -\left(\frac{p_{as}^{n+1} - p_{as}^{n}}{\Delta x}\right). \tag{23}$$

Term 1 should balance the other $\sigma(\partial p/\partial x)$ term (in the vector $A_\sigma$) that is treated implicitly and which is finite-differenced as follows:

$$\left(-|\sigma|\frac{\partial p}{\partial x}\right)_{\text{implicit}} = -|\sigma|\frac{p^{n+1} - p^{n}}{\Delta x}. \tag{24}$$

Therefore, term 1 must be evaluated by an expression that is as close as possible to Eq. (24). This expression is as follows:

$$-|\sigma|\frac{\partial p}{\partial x} = -|\sigma|\frac{p_{as}^{n+1} - p^{n}}{\Delta x}. \tag{25}$$

Since term 1 must be on the right-hand side, it cannot depend on $p^{n+1}$, and hence, $p_{as}^{n+1}$ is used.

Using Eqs. (23) and (25) in Eq. (22), the following expression for $S$ is obtained:

$$S = \left[0,\ -|\sigma|\frac{p_{as}^{n+1} - p^{n}}{\Delta x} - \frac{p_{as}^{n+1} - p_{as}^{n}}{\Delta x},\ 0\right]. \tag{26}$$

However, since Eq. (25) is different from Eq. (24), an inconsistency exists in the $x$-momentum equation. In order to study this inconsistency, the $x$-momentum equation is written as follows:

$$\cdots \quad -|\sigma|\frac{\partial p}{\partial x}\Big)_{\text{implicit}} = -|\sigma|\frac{\partial p}{\partial x}\Big)_{\text{explicit}} - \frac{\partial p}{\partial x}\Big)_{\text{explicit}} \tag{27}$$

other terms in $x$ momentum | term in $\partial A_\sigma/\partial x$ | terms in $S$

The above equation shows that the real $\partial p/\partial x$ is given by the following expression:

$$\frac{\partial p}{\partial x}\Big)_{\text{real}} = -|\sigma|\frac{\partial p}{\partial x}\Big)_{\text{implicit}} + |\sigma|\frac{\partial p}{\partial x}\Big)_{\text{explicit}} + \frac{\partial p}{\partial x}\Big)_{\text{explicit}} \tag{28}$$

$$p_{\text{real}}^{n+1} - p_{\text{real}}^{n} = -|\sigma|(p^{n+1} - p^{n}) + |\sigma|(p_{as}^{n+1} - p^{n}) + p_{as}^{n+1} - p_{as}^{n} \tag{29}$$

or

$$p_{\text{real}}^{n+1} = p_{\text{real}}^{n} - |\sigma|\, p^{n+1} + (|\sigma| + 1)\, p_{as}^{n+1} - p_{as}^{n}. \tag{30}$$

Equation (30) shows that the scheme becomes consistent only when the flow field

is swept several times, and $p_{as}$ is the pressure obtained from the previous sweep. When the solution converges, $p = p_{as}$ and $|\sigma| p_{as}^{n+1}$ cancels $-|\sigma| p^{n+1}$.

In the duct flows computed in this paper, the elliptic information is given in the prescription of the mass flow. Hence, one sweep is adequate. But when the elliptic effects are large, the convergency of pressure is not assured with a multisweep. In such a situation, either the pressure field must be known accurately or an iterative Poisson solver for the pressure must be introduced to obtain the pressure field.

The present study is concerned only with the single-sweep approach. The present method can be used in a single-sweep mode to predict parabolic flows in which the pressure gradient in the transverse plane does not depend on the streamwise direction. In other words, for $x$, $y$ Cartesian coordinates:

$$\frac{\partial p}{\partial y} \neq f(x). \tag{31}$$

When Eq. (31) holds, the inconsistency in the $x$-momentum equation does not affect the solution of the velocity field and the values of $\partial p/\partial y$. However, after the solution is completed, the pressure must be corrected through Eq. (30).

As will be seen later, the method gives good predictions even when Eq. (31) is not strictly valid. In other words, the method can be used in flows in which the transverse pressure gradient is a mild function of the streamwise direction.

Before closing this section, it must be mentioned that the present method is free from stability limitations associated with the minimum value of $\Delta x$. This limitation associated with many space-marching methods is absent in the present method because of the careful treatment of the eigenvalues. This has been confirmed through numerical experimentation. In one of these experients, the flow through a channel was calculated with 10,000 grid points in the streamwise direction per channel width. No instability was observed.

Another problem that should be addressed here is the choice of a value for $\sigma$. The value of $\sigma$ should not be very small, since as $\sigma$ tends to zero, the Jacobian matrix of the streamwise flux vector tends to become singular. It was found through numerical experimentation that the value of $\sigma$ should lie between 0.05 and 0.005. The value $\sigma = 0.01$ was used in all the computations presented in this paper.

## Extension to 3-Dimensional Flows

The extension of the method to three dimensions is straightforward. The $z$-momentum equation is added to the set of equations, and Eq. (16) takes the following form:

$$\frac{\partial A_\sigma(q)}{\partial x} + \frac{\partial B(q)}{\partial y} + \frac{\partial C(q)}{\partial z} = + \frac{1}{R_e}\left[\frac{\partial^2 D(q)}{\partial y^2} + \frac{\partial^2 E(q)}{\partial z^2}\right] + S \tag{32}$$

where $q$ is given by $q = [p, u, v, w]$, $w$ is the velocity component in $z$ direction.

The eigenvalues of $A_{\sigma J}^{-1} D_J$ and $A_{\sigma J}^{-1} E_J$ are as follows:

$$\lambda_{1,2} = 0; \qquad \lambda_{3,4} = 1/u. \tag{33}$$

The eigenvalues of $A_{\sigma J}^{-1} B_J$ are as follows:

$$\lambda_{1,2} = \pm \frac{1}{\sqrt{|\sigma|}}; \qquad \lambda_{3,4} = \frac{v}{u}. \tag{34}$$

And the eigenvalues of $A_{\sigma J}^{-1} C_J$ are as follows:

$$\lambda_{1,2} = \pm \frac{1}{\sqrt{|\sigma|}}; \qquad \lambda_{3,4} = \frac{w}{u}. \tag{35}$$

As with the 2-dimensional equations, Eq. (32) can be space marched in the streamwise direction $x$, as long as $u > 0$.

*Transformed Equations*

The boundary conditions are most easily and accurately implemented when the boundaries of the flow domain are constant-coordinate surfaces. Therefore, a body-fitted coordinate system is used in the physical domain. A transformation is used that maps the body-fitted grid in transforming the physical domain to a square grid in the computational domain (a cube). The transformation that connects the two domains can be written in the following form:

$$\begin{aligned} \xi &= \xi(x, y, z) \\ \eta &= \eta(x, y, z) \\ \zeta &= \zeta(x, y, z) \end{aligned} \tag{36}$$

where $\xi$ is the coordinate in the predominant flow direction, and $\eta$ and $\zeta$ are the coordinates in the transverse plane.

The equations in the physical domain are the steady non-dimensionalized Navier–Stokes equations for incompressible flow, given by

$$\frac{\partial A(q)}{\partial x} + \frac{\partial B(q)}{\partial y} + \frac{\partial C(q)}{\partial z} = \frac{1}{R_e}\left[\frac{\partial F(q)}{\partial x} + \frac{\partial D(q)}{\partial y} + \frac{\partial E(q)}{\partial z}\right] \tag{37}$$

where

$$A = \begin{bmatrix} u \\ u^2 + p \\ uv \\ uw \end{bmatrix}; \qquad B = \begin{bmatrix} v \\ vu \\ v^2 + p \\ vw \end{bmatrix}; \qquad C = \begin{bmatrix} w \\ wu \\ wv \\ w^2 + p \end{bmatrix}$$

$$F=\begin{bmatrix} 0 \\ 2\mu\dfrac{\partial u}{\partial x} \\ \mu\left(\dfrac{\partial v}{\partial x}+\dfrac{\partial u}{\partial y}\right) \\ \mu\left(\dfrac{\partial w}{\partial x}+\dfrac{\partial u}{\partial z}\right) \end{bmatrix}; \quad D=\begin{bmatrix} 0 \\ \mu\left(\dfrac{\partial u}{\partial y}+\dfrac{\partial v}{\partial x}\right) \\ 2\mu\left(\dfrac{\partial v}{\partial y}\right) \\ \mu\left(\dfrac{\partial w}{\partial y}+\dfrac{\partial v}{\partial z}\right) \end{bmatrix}; \quad E=\begin{bmatrix} 0 \\ \mu\left(\dfrac{\partial u}{\partial z}+\dfrac{\partial w}{\partial x}\right) \\ \mu\left(\dfrac{\partial v}{\partial z}+\dfrac{\partial w}{\partial y}\right) \\ 2\mu\dfrac{\partial w}{\partial z} \end{bmatrix}.$$

In the above equation, the molecular viscosity $\mu$ has been kept inside the derivative sign in order to be able to use the formulation in both the laminar and the turbulent flows. The molecular viscosity is replaced by the sum of the molecular and the eddy viscosity when the flow is turbulent.

The transformed equations in the computational domain can be cast in many different forms. Shamroth and Gibeling [14] have performed a detailed study of the different forms of the transformed equations. They found that the commonly used divergence form, in which all the fluxes and the metric coefficients are under derivative signs, introduces large truncation errors. This is because some flow variables (e.g., $p$) in some regions of the flow change from grid point to grid point in the fourth significant figure, whereas metric coefficients change in the second significant figure. As a result, flow variable changes are commensurate with the metric coefficient truncation error.

Shamroth and Gibeling suggested that a form in which the metric coefficients are kept outside of the derivative signs and the fluxes are kept inside gave the best results. Therefore, in the present study, Shamroth and Gibeling's suggestion is followed. According to the above discussion, Eq. (37) is written in the transformed coordinates in the following form:

$$\begin{aligned} &\xi_x\frac{\partial A}{\partial \xi}+\xi_y\frac{\partial B}{\partial \xi}+\xi_z\frac{\partial C}{\partial \xi}+\eta_x\frac{\partial A}{\partial \eta}+\eta_y\frac{\partial B}{\partial \eta}+\eta_z\frac{\partial C}{\partial \eta} \\ &\quad+\zeta_x\frac{\partial A}{\partial \zeta}+\zeta_y\frac{\partial B}{\partial \zeta}+\zeta_z\frac{\partial C}{\partial \zeta} \\ &=\frac{1}{R_e}\left[\xi_x\frac{\partial \hat{F}}{\partial \xi}+\xi_y\frac{\partial \hat{D}}{\partial \xi}+\xi_z\frac{\partial \hat{E}}{\partial \xi}+\eta_x\frac{\partial \hat{F}}{\partial \eta}+\eta_y\frac{\partial \hat{D}}{\partial \eta}+\eta_z\frac{\partial \hat{E}}{\partial \eta}\right. \\ &\quad\left.+\zeta_x\frac{\partial \hat{F}}{\partial \zeta}+\zeta_y\frac{\partial \hat{D}}{\partial \zeta}+\zeta_z\frac{\partial \hat{E}}{\partial \zeta}\right]. \end{aligned} \tag{38}$$

In the above expression, $\xi_x$, $\xi_y$, $\xi_z$, $\eta_x$, $\eta_y$, $\eta_z$, $\zeta_x$, $\zeta_y$, $\zeta_z$ are the metric coefficients. The Vectors $F$, $D$, $E$ are the transformed $\hat{F}$, $\hat{D}$, $\hat{E}$ vectors, respectively.

In order to be able to solve Eq. (38) by space marching in the $\xi$ direction, the

viscous diffusion terms in this direction are dropped, and the flux vectors $A$, $B$, and $C$ under a $\xi$ derivative are split as follows:

$$A_\sigma = \begin{bmatrix} u \\ u^2 - |\sigma| p \\ uv \\ uw \end{bmatrix}; \quad A_p = \begin{bmatrix} 0 \\ |\sigma| p + p \\ 0 \\ 0 \end{bmatrix}; \quad B_\sigma = \begin{bmatrix} v \\ vu \\ v^2 - |\sigma| p \\ vw \end{bmatrix}$$

$$B_p = \begin{bmatrix} 0 \\ 0 \\ |\sigma| p + p \\ 0 \end{bmatrix}; \quad C_\sigma = \begin{bmatrix} w \\ uw \\ vw \\ w^2 - |\sigma| p \end{bmatrix}; \quad C_p = \begin{bmatrix} 0 \\ 0 \\ 0 \\ |\sigma| p + p \end{bmatrix}$$

With these modifications, Eq. (38) takes the following form:

$$\begin{aligned} &\xi_x \frac{\partial A_\sigma}{\partial \xi} + \xi_y \frac{\partial B_\sigma}{\partial \xi} + \xi_z \frac{\partial C_\sigma}{\partial \xi} \\ &\quad = -\eta_x \frac{\partial A}{\partial \eta} - \eta_y \frac{\partial B}{\partial \eta} - \eta_z \frac{\partial C}{\partial \eta} - \zeta_x \frac{\partial A}{\partial \zeta} - \zeta_y \frac{\partial B}{\partial \zeta} - \zeta_z \frac{\partial C}{\partial \zeta} \\ &\qquad - \xi_x \frac{\partial A_p}{\partial \xi} - \xi_y \frac{\partial B_p}{\partial \xi} - \xi_z \frac{\partial C_p}{\partial \xi} \\ &\qquad + \frac{1}{R_e}\left[\eta_x \frac{\partial \bar{F}}{\partial \eta} + \eta_y \frac{\partial \bar{D}}{\partial \eta} + \eta_z \frac{\partial \bar{E}}{\partial \eta} + \zeta_x \frac{\partial \bar{F}}{\partial \zeta} + \zeta_y \frac{\partial \bar{D}}{\partial \zeta} + \zeta_z \frac{\partial \bar{E}}{\partial \zeta}\right]. \end{aligned} \tag{40}$$

The vectors $\bar{F}$, $\bar{D}$, and $\bar{E}$ are derived by dropping the terms involving $\partial/\partial\xi$ in $F$, $D$, and $E$, respectively.

*The Numerical Algorithm for the 3D Transformed Equation*

The numerical algorithm used in this study is based on Beam and Warming's [15] and Briley and McDonald's [16] implicit factored schemes. The vectors $\bar{F}$, $\bar{D}$, $\bar{E}$, are split as follows:

$$\begin{aligned} \bar{F} &= \bar{F}_1 + \bar{F}_2 \\ \bar{D} &= \bar{D}_1 + \bar{D}_2 \\ \bar{E} &= \bar{E}_1 + \bar{E}_2. \end{aligned} \tag{41}$$

$\bar{F}_1$, $\bar{D}_1$, and $\bar{E}_1$ contain the terms under an $\eta$ derivative, and $\bar{F}_2$, $\bar{D}_2$, and $\bar{E}_2$, contain the terms under a $\zeta$ derivative.

For convenience, in presenting the numerical algorithm, the following definitions are introduced:

$$
\begin{aligned}
L_1 &= -\eta_x \frac{\partial A}{\partial \eta} - \eta_y \frac{\partial B}{\partial \eta} - \eta_z \frac{\partial C}{\partial \eta} + \frac{1}{R_e}\left[\eta_x \frac{\partial \bar{F}_1}{\partial \eta} + \eta_y \frac{\partial \bar{D}_1}{\partial \eta} + \eta_z \frac{\partial \bar{E}_1}{\partial \eta}\right] \\
L_2 &= -\zeta_x \frac{\partial A}{\partial \zeta} - \zeta_y \frac{\partial B}{\partial \zeta} - \zeta_z \frac{\partial C}{\partial \zeta} + \frac{1}{R_e}\left[\zeta_x \frac{\partial \bar{F}_2}{\partial \zeta} + \zeta_y \frac{\partial \bar{D}_2}{\partial \zeta} + \zeta_z \frac{\partial \bar{E}_2}{\partial \zeta}\right] \\
L_{12} &= \frac{1}{R_e}\left[\eta_x \frac{\partial \bar{F}_2}{\partial \eta} + \eta_y \frac{\partial \bar{D}_2}{\partial \eta} + \eta_z \frac{\partial \bar{E}_2}{\partial \eta} + \zeta_x \frac{\partial \bar{F}_1}{\partial \zeta} + \zeta_y \frac{\partial \bar{D}_1}{\partial \zeta} + \zeta_z \frac{\partial \bar{E}_1}{\partial \zeta}\right] \\
S &= -\xi_x \frac{\partial A_p}{\partial \xi} - \xi_y \frac{\partial B_p}{\partial \xi} - \xi_z \frac{\partial C_p}{\partial \xi}.
\end{aligned}
\tag{42}
$$

$L_1$ contains all the terms that involve only $\eta$ derivatives; $L_2$ contains all the terms that involve only $\zeta$ derivatives; $L_{12}$ contains all the terms that involve mixed derivatives; and $S$ contains the streamwise pressure gradient terms that are treated as known source terms, as discussed earlier.

Using Eq. (42) in Eq. (40), the following expression is obtained:

$$
\xi_x \frac{\partial A_\sigma}{\partial \xi} + \xi_y \frac{\partial B_\sigma}{\partial \xi} + \xi_z \frac{\partial C_\sigma}{\partial \xi} = L_1 + L_2 + L_{12} + S. \tag{43}
$$

A fully implicit (Euler implicit scheme) finite difference equivalent to Eq. (43) can be written in the following form:

$$
\xi_x(A_\sigma^{n+1} - A_\sigma^n) + \xi_y(B_\sigma^{n+1} - B_\sigma^n) + \xi_z(C_\sigma^{n+1} - C_\sigma^n) = \Delta\xi(L_1 + L_2 + L_{12} + S)^{n+1}. \tag{44}
$$

In the above expression, $\Delta\xi$ is the streamwise step size; $n$ is the index in the streamwise direction; $(n+1)$ is the streamwise location at which the solution is sought; and the solution is known at $(n)$.

Equation (44) is still non-linear and not in a form suitable for efficient numerical computation. The non-linear flux vectors at the level $(n+1)$ can be linearized by expanding them in a Taylor series about the level $n$:

$$
\begin{aligned}
A_\sigma^{n+1} &= A_\sigma^n + \left(\frac{\partial A_\sigma^n}{\partial q}\right)\Delta q^n; \; B_\sigma^{n+1} = B_\sigma^n + \left(\frac{\partial B_\sigma^n}{\partial q}\right)\Delta q^n \\
C_\sigma^{n+1} &= C_\sigma^n + \left(\frac{\partial C_\sigma^n}{\partial q}\right)\Delta q^n; \; L_1^{n+1} = L_1^n + \left(\frac{\partial L_1^n}{\partial q}\right)\Delta q^n \\
L_2^{n+1} &= L_2^n + \left(\frac{\partial L_2}{\partial q}\right)^n \Delta q^n.
\end{aligned}
\tag{45}
$$

The vector $L_{12}$ is going to be treated explicitly. This is because the mixed derivative terms cannot be separated into individual operators for the two-coor-

dinate directions in the cross flow, and, therefore, they are treated explicitly. As has been shown by Beam and Warming [17], treating the mixed derivative terms explicitly does not deteriorate the stability of the scheme. Therefore, $L_{12}$ is linearized as follows:

$$L_{12}^{n+1} = L_{12}^{n}. \tag{46}$$

The vector $S$ is being treated explicitly in a direct extension of Eq. (26):

$$S^{n+1} = -\left(|\sigma| \frac{p_{as}^{n+1} - p^{n}}{\Delta\xi} + \frac{p_{as}^{n+1} - p_{as}^{n}}{\Delta\xi}\right) \begin{bmatrix} 0 \\ \xi_x \\ \xi_y \\ \xi_z \end{bmatrix}. \tag{47}$$

The use of Eqs. (45), (46), and (47) in Eq. (44) gives the following linearized equation:

$$\left[\xi_x\left(\frac{\partial A_\sigma^n}{\partial q}\right) + \xi_y\left(\frac{\partial B_\sigma^n}{\partial q}\right) + \xi_z\left(\frac{\partial C_\sigma^n}{\partial q}\right)\right] \Delta q^n$$
$$= \Delta\xi[L_1 + L_2 + L_{12}]^n + S^{n+1} + \Delta\xi\left[\left(\frac{\partial L_1}{\partial q}\right)^n + \left(\frac{\partial L_2}{\partial q}\right)^n\right] \Delta q^n. \tag{48}$$

The rearrangement of Eq. (48) gives the following expression:

$$\left[\xi_x\left(\frac{\partial A_\sigma^n}{\partial q}\right) + \xi_y\left(\frac{\partial B_\sigma^n}{\partial q}\right) + \xi_z\left(\frac{\partial C_\sigma^n}{\partial q}\right) - \Delta\xi\left[\left(\frac{\partial L_1^n}{\partial q}\right) + \left(\frac{\partial L_2^n}{\partial q}\right)\right]\right] \Delta q^n$$
$$= \Delta\xi(L_1 + L_2 + L_{12})^n + S^{n+1}. \tag{49}$$

Equation (49) can be written in a compact form by naming the right-hand side of it $R$, and setting

$$\xi_x\left(\frac{\partial A_\sigma}{\partial q}\right)^n + \xi_y\left(\frac{\partial B_\sigma}{\partial q}\right)^n + \xi_z\left(\frac{\partial C_\sigma}{\partial q}\right)^n = W$$
$$-\Delta\xi\left(\frac{\partial L_1}{\partial q}\right)^n = Q_1$$
$$-\Delta\xi\left(\frac{\partial L_2}{\partial q}\right)^n = Q_2. \tag{50}$$

With the above definitions, Eq. (49) takes the following form:

$$(W + Q_1 + Q_2)\,\Delta q^n = R. \tag{51}$$

Using Douglas and Gunn's [18] split schemes, the above equation is factored as follows:

$$\begin{aligned}(W+Q_1)\,\Delta q^* &= R\\ (W+Q_2)\,\Delta q^n &= W\,\Delta q^*.\end{aligned} \tag{52}$$

Equation (52) represents a two-step factorized scheme that is fully implicit and unconditionally stable. The stability analysis of the scheme has been discussed by Warming and Beam [19] and Briley and McDonald [16]. Each of the steps in Eq. (52) involves the inversion of a block $(4\times 4)$ tridiagonal matrix.

*The Boundary Conditions*

The discretization of the governing equations, at any one of the half-steps in the factored algorithm, produces a block tridiagonal system of equations that can be written in the following form:

$$L_i\,\Delta q_{i-1} + D_i\,\Delta q_i + U_i\,\Delta q_{i+1} = R_i \tag{53}$$

where $L$, $D$, and $U$ are the lower diagonal, and upper diagonal block coefficient matrices and $R$ the right-hand side vector; $i$ is the index in the direction normal to the boundary. At the first grid point away from the boundary (say, the left boundary), Eq. (53) is written as follows:

$$L_1\,\Delta q_b + D_1\,\Delta q_1 + U_1\,\Delta q_2 = R_1. \tag{54}$$

The subscript $b$ refers to the values on the boundary. The change in the vector of unknowns $\Delta q_b$ on the boundary must be eliminated from the system of equations. This is done through the application of implicit boundary conditions. $\Delta q_b$ can be related to $\Delta q$ at the interior points or simply $\Delta q_b$ may be known. In the case that it is not known, it is calculated from the evaluated $\Delta q$ at the interior points. This is done through the application of the explicit boundary conditions. As will be shown later, sometimes it is necessary to employ different boundary conditions on the implicit and the explicit sides.

In a space-marching method, there is no need to specify downstream boundary conditions. Also, the upstream boundary conditions, referred to as initial conditions in the present study, are always specified. Therefore, only the boundary conditions on the remaining four sides of the domain are considered.

Many different types of boundaries can be found in fluid flows. Here, only two kinds of boundaries will be considered: (i) solid wall, and (ii) the boundary on which the solution is known.

*Boundary Conditions on Solid Walls*

In a flow over a solid wall, the no-slip condition for the velocities is used for both the implicit and the explicit side of the equations. The boundary condition on the pressure is $\partial p/\partial n = 0$, where $n$ is the direction normal to the wall. This condition is

enforced both on the implicit and the explicit side of the equations. It should be noted here that it is very important to enforce the normal boundary condition on the pressure ($\partial p/\partial n = 0$) implicitly. Also, the way it is implemented is very important. This is because this boundary condition is the only link between the pressure at the odd and even points. It is well known that, when a central difference scheme is used (as in the present method in the transverse plane), the pressures at the odd and even points tend to uncouple in the transverse plane and produce saw-like pressure solutions which generate saw-like secondary velocities; eventually, the computation becomes unstable. However, through the use of $\partial p/\partial n = 0$, it is possible to couple the grid point on the wall (an even point) with the first grid point away from the wall (an odd point). If this is done implicitly, it is possible to avoid the uncoupling of the pressure at the odd and the even points.

The question that should be answered now is what kind of difference must be used to approximate $\partial p/\partial n = 0$. An obvious choice is to use a second-order accurate forward-differencing:

$$\left.\frac{\partial p}{\partial n}\right|_b = \frac{-3p_b + 4p_1 - p_2}{2\Delta n} = 0 \tag{55}$$

where the subscript $b$ indicates the values on the boundary: (1) the values at the first grid point away from the wall; and (2) the values at the second point away from the wall. However, in many cases, Eq. (55) did not prevent the pressure solution from uncoupling.

Another way of differencing $\partial p/\partial n$ is by using a first-order accurate forward expression:

$$\left.\frac{\partial p}{\partial n}\right|_b = \frac{-p_b + p_1}{\Delta n} = 0. \tag{56}$$

Equation (56), even though less accurate than Eq. (55), always provided better coupling of the pressure at the odd and even points. The explanation for this is simple. When Eq. (56) is used, the value of $p$ at the boundary point (an even point) is determined exclusively by the value of $p$ at the first grid point away from the wall (an odd point). However, when Eq. (55) is used, the value of $p$ at the boundary is also influenced by the value of $p$ at the second grid point away from the wall, which is also an even point, and, thus, the coupling of odd and even points is reduced.

*Boundary Conditions for Boundaries on Which the Solution Is Known*

At first thought, it seems that there should be no problem in applying boundary conditions on boundaries on which the solution is known. This is true as far as the velocities are concerned. However, this is not true for the pressure. If the known pressure on the boundary is used both on the implicit and the explicit side of the equations, the solution for the pressure at the odd and even points quickly uncouples. To avoid the problem, the normal boundary condition for the pressure

$\partial p/\partial n = 0$ is used on the implicit side of the equations. On the explicit side, the correct value of $p$ is used on the boundary.

The known values of the velocities are used both on the implicit and the explicit sides of the equations.

## Method and Code Verification

In order to check the method and the computer code written to implement it, several test cases were computed, and the results were compared with the available exact solutions and the experimental data. Since the primary objective for running these cases was to check the technique, the flows were chosen to be laminar in order to avoid any inaccuracies arising from the turbulence model. Also, the geometry was chosen to be simple in order to avoid any problems arising from the grid.

### *Developing Laminar Flow in a 2D Channel*

One of the test cases computed was the developing laminar flow in a 2-dimensional channel. Even though this test case is a simple one, it will show some of the important features of the method. It will indicate whether or not the method con-

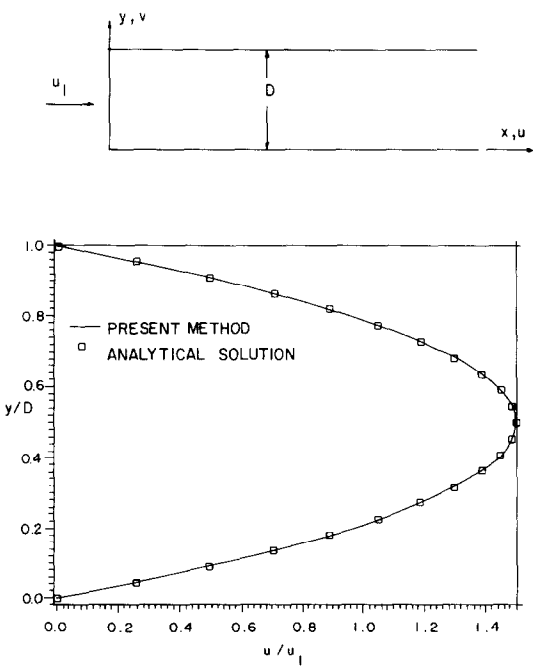


FIG. 1. Fully developed laminar flow through a 2D channel.

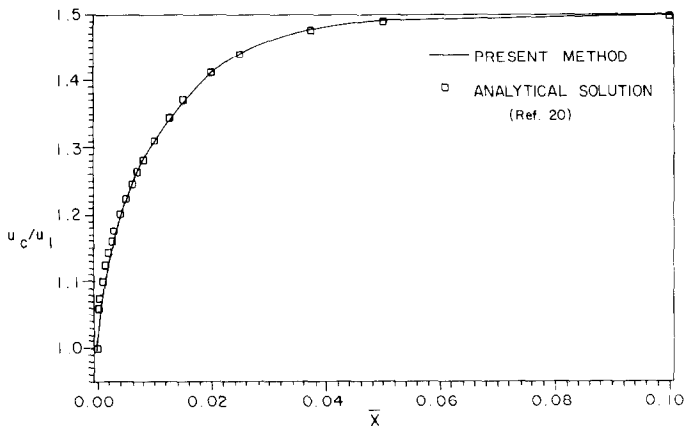


FIG. 2. Centerline velocity of the laminar flow through a 2D channel.

serves the mass, and also how the method reacts to the assumed streamwise pressure gradient.

A Cartesian grid was used in the physical domain, with constant spacing in both the axial and the transverse directions. Twenty-one points were used in the transverse direction, and 20 points per width in the streamwise direction. The Reynolds number, based on the width of the domain, was chosen to be equal to 500. At the entrance of the channel, a uniform flow was specified as the initial velocity profile ($u_1 = 1$). The transverse velocity and the pressure were set equal to zero at the initial station.

The predicted, fully developed streamwise velocity profile is compared with the analytical solution (parabolic profile) in Fig. 1. The agreement between the two is

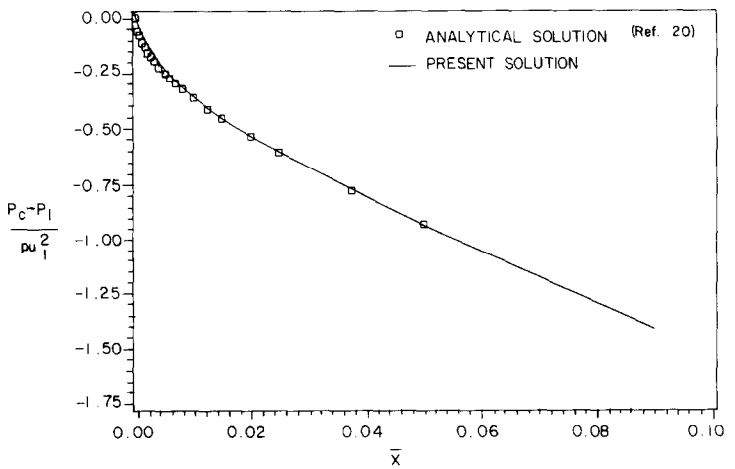


FIG. 3. Centerline pressure of the laminar flow through a 2D channel.

excellent. This demonstrates the ability of the method to conserve the mass flow. Note that this was achieved with no extra computation. In all other subsonic space-marching or parabolic methods, some kind of adjustment is needed after each step to ensure mass conservation.

In order to check whether the method accurately predicts the developing part of the flow, the centerline streamwise velocity $u_c$ is plotted in Fig. 2 vs the scaled streamwise distance $\bar{X}$, where $\bar{X} = (x/D)/R_{eD}$; $D$ is the width of the channel; and $R_{eD} = (u_1 D)/v$. In the same figure, the analytical results of Schlichting [20] are also plotted. The agreement between the two is very good.

The predicted centerline pressure versus the scaled streamwise distance is compared with that from the analytical solution of Schlichting in Fig. 3. In this figure $P_1$ is the inlet pressure, $P_c$ is the pressure along the centerline. Again the agreement between the two is very good. This shows that the present method can predict the streamwise pressure gradient accurately (at least for simple parabolic flows).

This, however, sounds surprising since the incompressible fluid flow is an elliptic phenomenon. Therefore, there is no way to predict the pressure and velocity fields accurately by just sweeping the flow field once without any "elliptic information" transmitted upstream through multiple sweeps of the flow field. This argument is correct. The only reason that the method gives an accurate prediction of the flow field in a single sweep is that "elliptic information" is indeed given to the set of equations. This "elliptic information" is coming through the initial velocity profile.

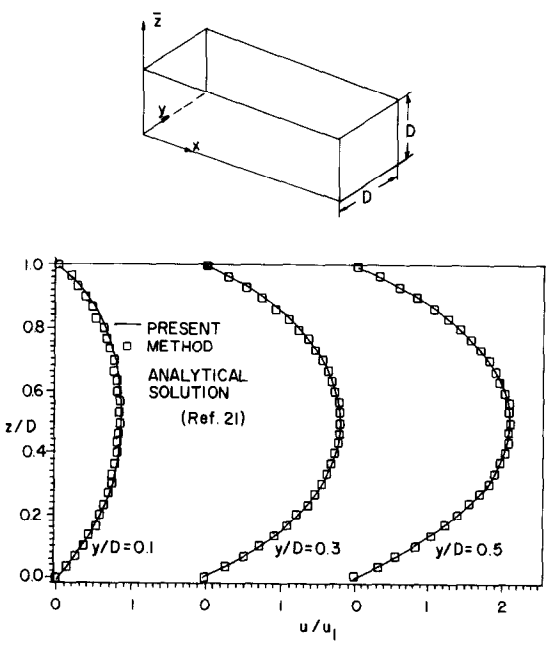


FIG. 4. Fully developed laminar flow through a square, straight duct.

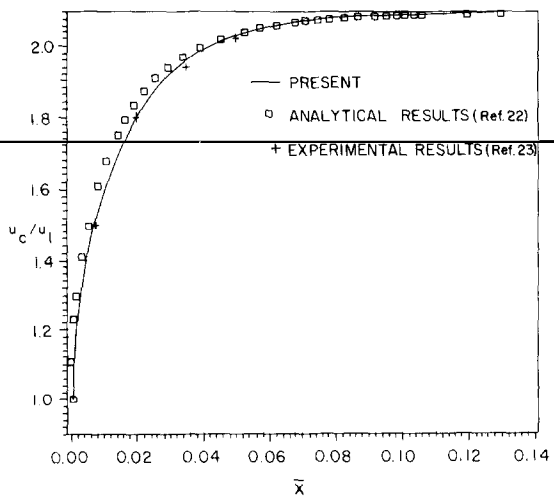


FIG. 5. Centerline velocity of the laminar flow through a square, straight duct.

When the initial velocity profile is specified at the initial plane, the total mass flow through the channel is specified. This specified total mass flow contains all the necessary "elliptic information" that a method needs for the accurate prediction of the flow field through a constant area channel. In the next sections, it will be shown that this is also true for 3-dimensional ducts with constant area and curvature.

*Developing Laminar Flow in a Square, Straight Duct*

This flow is similar to the 2-dimensional channel flow studied in the previous section, but with the added complication that the flow is developing in a 3-dimensional geometry.

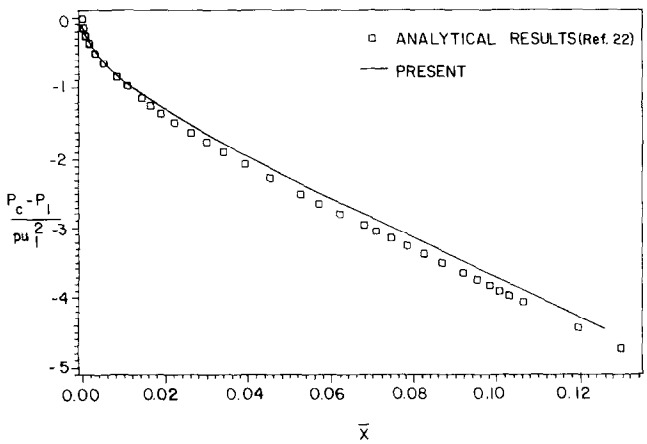


FIG. 6. Centerline pressure of the laminar flow through a square, straight duct.

A Cartesian grid was used in the physical domain with constant spacing in all three directions. Twenty-one points were used in each of the transverse directions, and 20 points per width in the streamwise direction. The Reynolds number, based on the width of the duct, was chosen to be equal to 500. At the entrance of the duct, a uniform flow was specified as the initial velocity profile ($u_1 = 1$). The transverse velocities and the pressures were set equal to zero at the initial station.

The predicted, fully developed streamwise velocity profiles at $y/D = 0.1$, 0.3, and 0.5 are compared with the analytical solution (see White [21]) in Fig. 4. The agreement between them is very good.

The predicted centerline velocity is compared with the analytical results of Han [22], and with the experimental data of Goldstein and Kreid [23] in Fig. 5. The agreement between them is likewise very good.

The predicted centerline pressure is compared with the analytical solution of Han in Fig. 6. Again, the agreement between them is very good.

Note that the present method captures the effects of the entrance region of the duct accurately. The rapid acceleration of the core flow in the entrance region of the duct results in a sharp drop of the pressure. The acceleration of the flow and the pressure drop decreases as the flow develops downstream. The pressure drop becomes eventually linear in the fully developed region. All of these features are accurately predicted.

As with the flow through the 2-dimensional channel, the solution through the square duct was obtained in a single sweep. The solution was started with $p_{as} = 0$.

In both the 2-dimensional channel case and the straight square duct case, the transverse pressure gradient does change with the streamwise direction in the entrance region. However, the method was able to give excellent predictions since the magnitude of the transverse pressure gradient is small.

*Developing Laminar Flow in a Square, Curved Duct*

The laminar flow through a mildly curved square duct was first computed. The ratio of the radius of curvature to the width of that duct was 14.5 ($R_c/D = 14.5$).

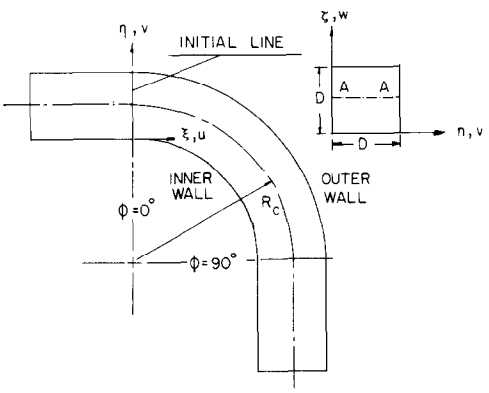


FIG. 7. Geometry of a square, curved duct.

The prediction of the present method agreed very well with Ghia and Sokhey's [24] numerical results for the same duct. However, the strength and the limitations of a space-marching (or parabolic) method become apparent only when it is used to predict flows through strongly curved ducts.

Taylor, Whitelaw, and Yianneskis [25] measured the laminar ($R_{eD} = 790$) flow through a strongly curved duct with constant area. The ratio of the radius of cur-

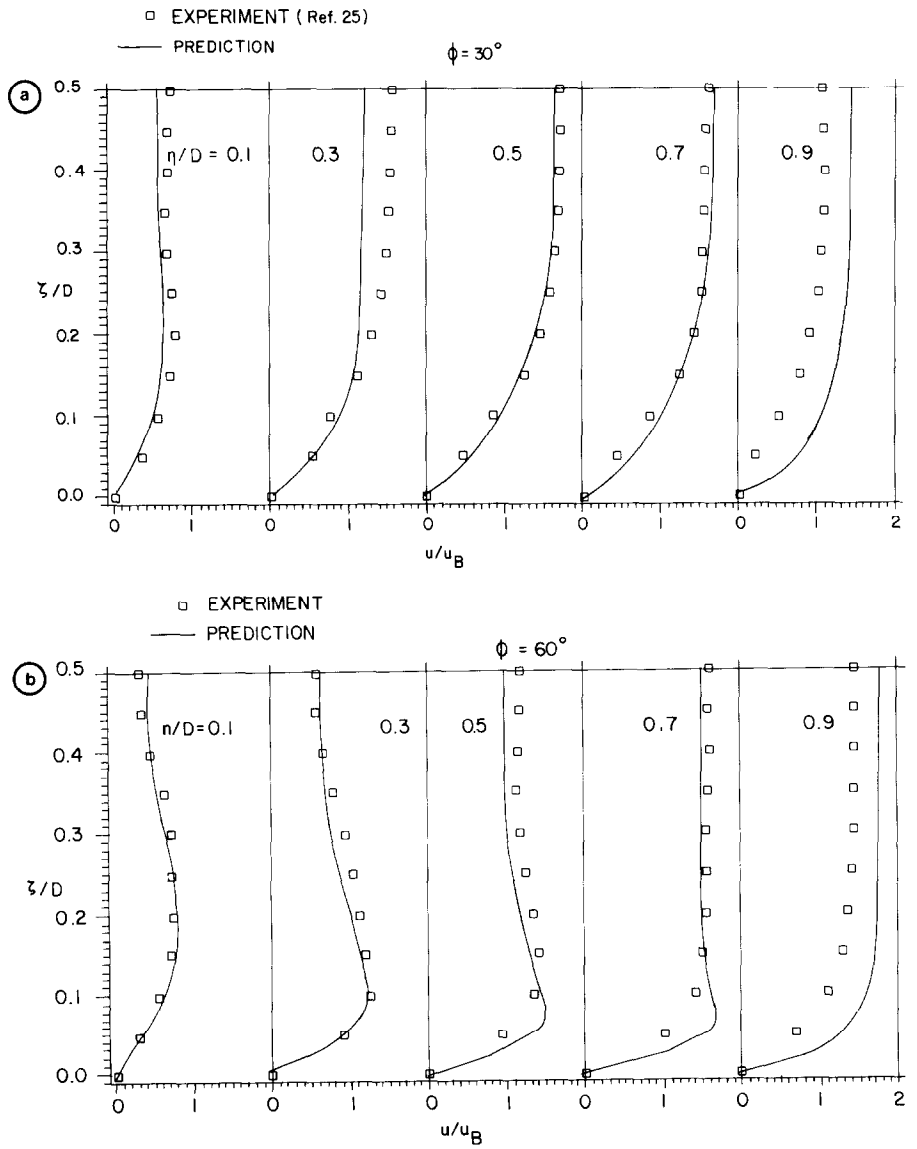


FIG. 8. Streamwise velocity profiles (a) at $\phi = 30°$; (b) at $\phi = 60°$; (c) at $\phi = 77.5°$.

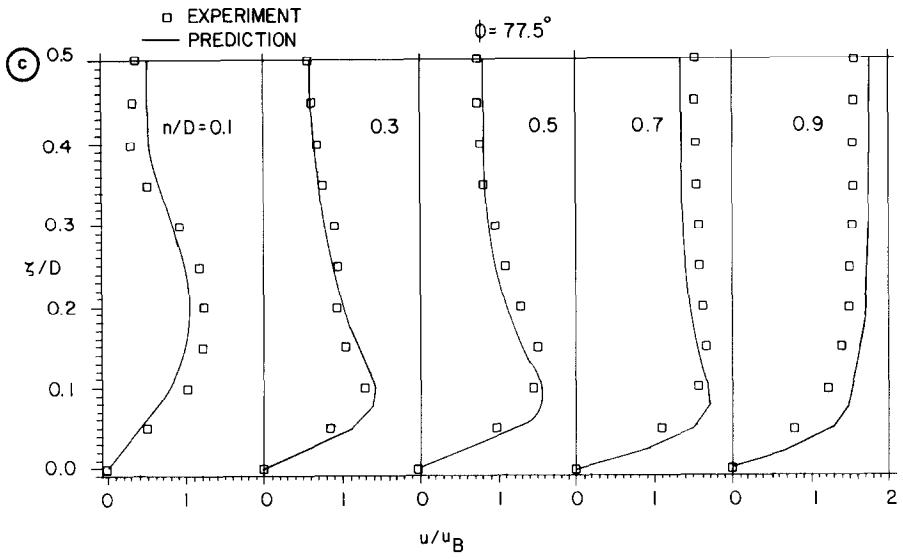


FIG. 8—*Continued.*

vature to the width of the duct was 2.3 ($R_c/D = 2.3$). The turning of the duct was 90° (see Fig. 7). The curvature of the duct was zero upstream of the location with $\phi = 0°$, and downstream of the location with $\phi = 90°$. At the inlet of the bend ($\phi = 0°$), the flow was partly developed, with the boundary layer thickness being approximately 25% of the duct width. In this duct, very strong secondary velocities were generated, reaching 60% of the bulk velocity.

The computation for this duct was started at $\phi = 0°$ (or $\xi/D = 0$). The velocity profile at the inlet plane was obtained from the available experimental data through interpolation. The assumed pressure was approximated at the horizontal centerline *A–A* (Fig. 7) through the simple radial equilibrium equation, and it was assumed constant in the spanwise and streamwise directions.

The computation was carried out only in the lower half of the duct (from $\zeta/D = 0$ to $\zeta/D = 0.5$), since the flow is symmetric about the horizontal centerline *A–A*. Forty-one grid points were used in the $\eta$-direction; 21 grid points, in the $\zeta$-direction; and 180 streamwise stations, between $\phi = 0°$ and $\phi = 90°$. The computed streamwise velocity $u$, normalized by the bulk velocity $u_B$, is compared to the measured velocity $u$ at three streamwise locations ($\phi = 30°$, 60°, 77.5°) in Figs. 8a, b, and c. Each figure shows the velocity profiles at five different locations ($\eta/D = 0.1$, 0.3, 0.5, 0.7, 0.9) plotted against the spanwise direction $\zeta$. The $u$ component of velocity is along the $\xi$ coordinate (see Fig. 7). The agreement between predictions and measurements is good at most locations. Note that the method captures the large distortions of the streamwise velocity (e.g., see the profile at $\phi = 77.5°$, $\eta/D = 0.3$ in Fig. 8c). This distortion is due to the large secondary velocities that develop in the transverse plane.

The computed secondary velocity $v$, normalized by the bulk velocity $u_B$, is compared to the measured velocity $v$ in Figs. 9a, b, and c. The $v$ component of velocity is along the $\eta$ coordinate (see Fig. 7). The agreement between predictions and measurements is good at most locations. The method captures the peak value of $v$ ($=0.6u_B$) and all the qualitative features of the flow (e.g., see the profile at $\phi = 60°$, $\eta/D = 0.1$ in Fig. 9b). The secondary velocity vectors ($|Q_s| = \sqrt{v^2 + w^2}$) in the $\eta - \zeta$

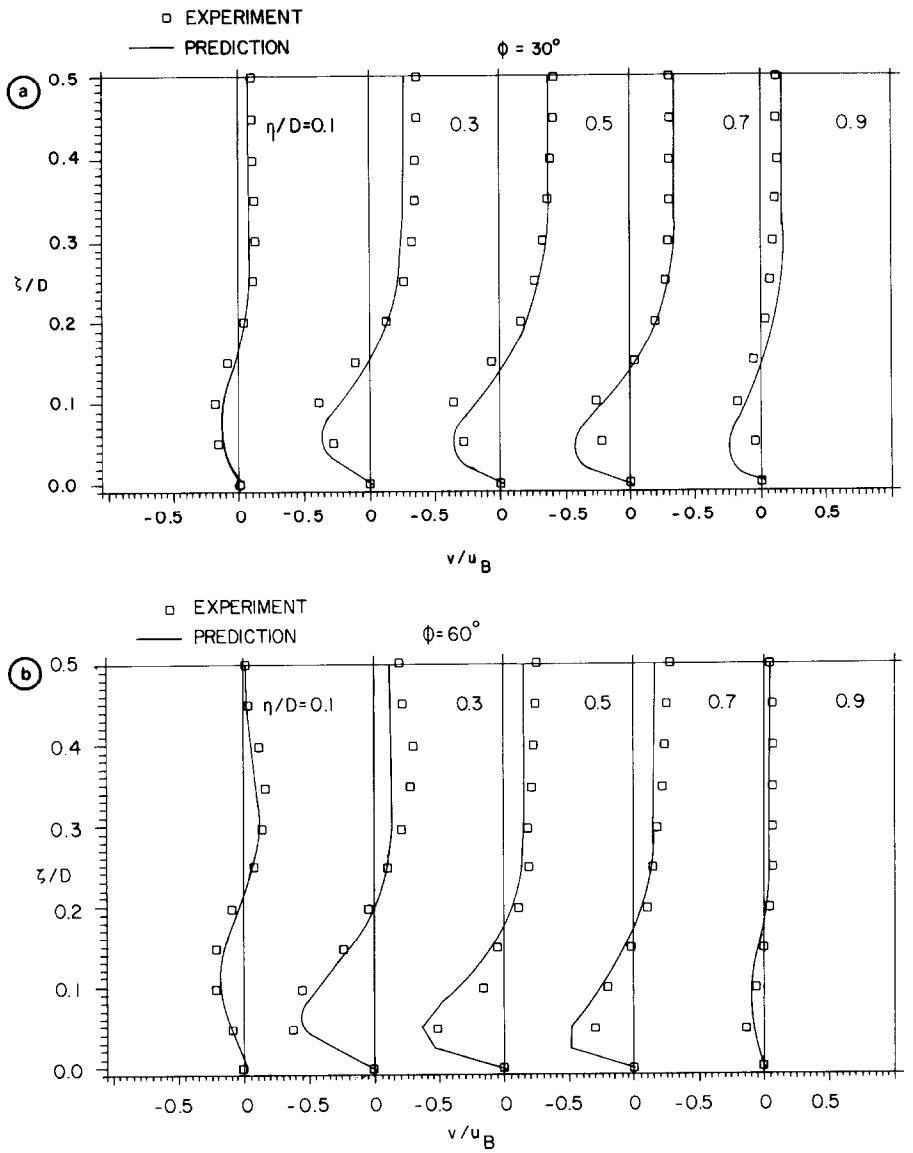


FIG. 9. Secondary velocity profiles (a) at $\phi = 30°$; (b) at $\phi = 60°$; (c) at $\phi = 77.5°$.

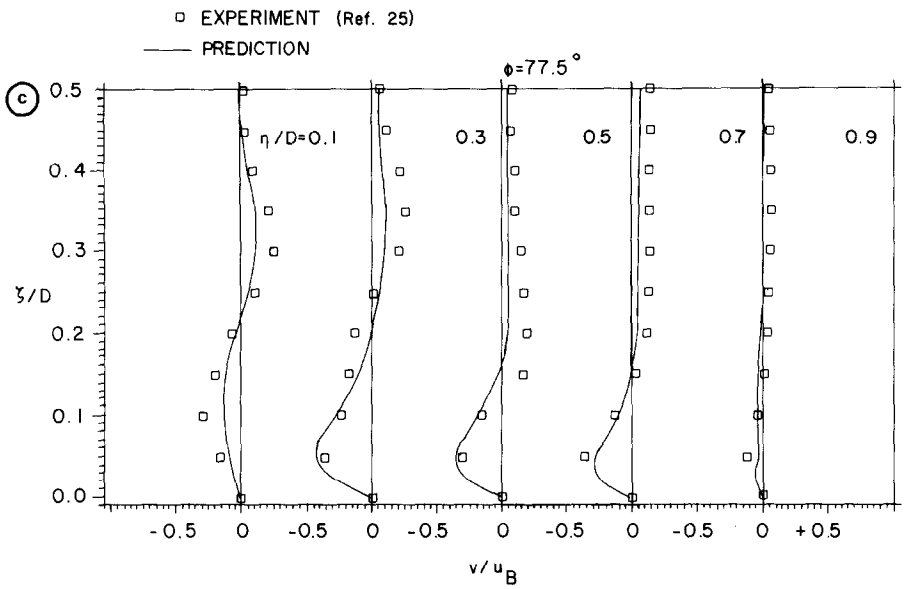


FIG. 9—*Continued.*

plane at $\phi = 30°$, 60°, and 77.5° are shown in Figs. 10a, b, and c, respectively. It can be seen that, while going from $\phi = 30°$ to $\phi = 77.5°$, the vortex becomes stronger and moves towards the inner wall and the horizontal centerline $A$–$A$.

As with the previous cases, the solution through square curved ducts was obtained in a single sweep. In this test case, the transverse pressure gradient is strong, but it is not changing rapidly in the streamwise direction. This test case showed that this technique is adequate for flows with strong transverse pressure gradients which are weakly dependent on the streamwise direction.

## CONCLUDING REMARKS

A space-marching method for steady incompressible flow has been developed that can accurately predict both the velocity and the pressure field in parabolic flows such as the flows through straight and curved ducts with constant area and curvature. The method can capture strong secondary flows, and the streamwise and the transverse pressure gradients. It should be mentioned here that all the results were obtained without any artificial damping (or dissipation), even though the method employs a central difference scheme in the transverse plane. This shows the effectiveness of the normal boundary condition on the pressure ($\partial p/\partial n = 0$) in

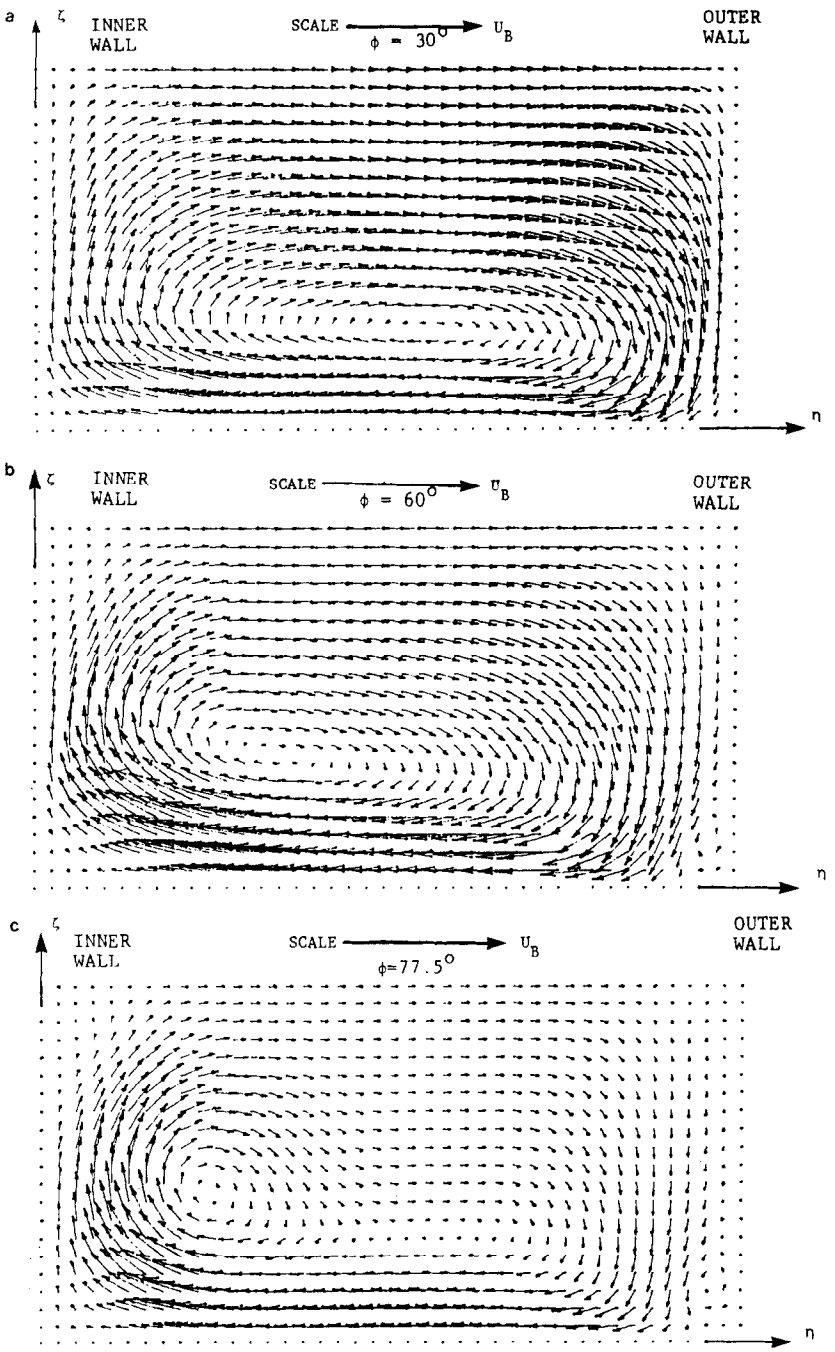


FIG. 10. Secondary velocity vectors (a) ($\vec{Q}_s$) at $\phi = 30°$ (laminar flow); (b) ($\vec{Q}_s$) at $\phi = 60°$ (laminar flow); (c) ($\vec{Q}_s$) at $\phi = 77.5°$ (laminar flow).

parabolic flows, like the flows through ducts, without the help of an assumed pressure field. The only information needed by the method is the geometry of the flow domain and the inlet velocity profile. The latter contains the necessary "elliptic information," as explained earlier.

The reader must be warned that, for more complex flow fields where the elliptic effects are significant, accurate prescription of the pressure field or an iterative solver for the pressure field is essential. Also, the method, as it stands now, cannot be applied to external flows, where the mass flow constraint is absent.

## ACKNOWLEDGMENTS

This work was sponsored by NASA, under Grant NSG 3266, with Dr. P. Sockol as the Technical Monitor. The computational time was provided by The Pennsylvania State University. The authors wish to express their thanks to the anonymous reviewers, whose useful comments have been incorporated in the paper.

## REFERENCES

1. S. V. PATANKAR AND D. B. SPALDING, *Int. J. Heat Transfer* **15**, 1787 (1972).
2. W. R. BRILEY, *J. Comput. Phys.* **14**, No. 1, 8 (1974).
3. U. GHIA, K. N. GHIA, AND C. J. STUDERUS, *Comput. Fluids* **5**, (1977).
4. J. MOORE AND J. G. MOORE, *J. Fluids Eng.* **101**, 415 (1979).
5. R. CHILUKURI AND R. H. PLETCHER, *Numer. Heat Transfer* **3**, 169 (1980).
6. W. R. BRILEY AND H. MCDONALD, *J. Fluid Mech.* (1984).
7. T. C. LIN AND S. G. RUBIN, *Comput. Fluids* **1**, 37 (1973).
8. H. MCDONALD AND W. R. BRILEY, *J. Comput. Phys.* **19**, 150 (1975).
9. Y. C. VIGNERON, J. V. RAKICH, AND J. C. TANNEHILL, "Calculation of Supersonic Viscous Flow Over Delta Wings With Sharp Subsonic Leading Edges," AIAA Paper 78-1137, 1978.
10. S. C. LUBARD AND W. S. HELLIWELL, *AIAA J.* **12**, No. 7, 965 (1974).
11. L. B. SCHIFF AND J. L. STEGER, *AIAA J.* **18**, No. 12, 1421 (1980).
12. T. R. GOVINDAN, "A Space-Marching Method for the Navier–Stokes Equations for Internal Flows," Ph. D. thesis, Aerospace Engineering, Pennsylvania State University, 1983.
13. J. V. RAKICH, "Iterative PNS Method for Attached Flows with Upstream Influence," AIAA Paper 83-1955, 1983.
14. S. J. SHAMROTH AND H. J. GIBELING, "A Compressible Solution for the Navier–Stokes Equations for Turbulent Flow about an Airfoil," NASA CR-3183, 1979.
15. R. BEAM AND R. F. WARMING, *AIAA J.* **16**, 393 (1978).
16. W. R. BRILEY AND H. MCDONALD, *J. Comput. Phys.* **34**, 54 (1980).
17. R. BEAM AND R. F. WARMING, *SIAM Sci. Statist. Comput.* **1**, No. 1, 131 (1980).
18. J. DOUGLAS AND J. E. GUNN, *Numer. Math.* **6**, 428 (1980).
19. R. F. WARMING AND R. BEAM, in *SIAM-AMS Proceedings, Vol. 11, Proceedings of the Symposium on Computational Fluid Mechanics*, New York, 1977.
20. H. SCHLICHTING, *Boundary Layer Theory*, 4th ed., McGraw–Hill, New York, 1960.
21. F. M. WHITE, *Viscous Fluid Flow*, McGraw–Hill, New York, 1974.
22. L. S. HAN, *J. Appl. Mech.* **27**, No. 3, 403 (1960).
23. R. J. GOLDSTEIN AND D. K. KREID, *J. Appl. Mech.* **34**, No. 4, 813 (1967).
24. K. N. GHIA AND J. S. SOKHEY, *J. Fluids Eng.* **99**, 640 (1977).
25. A. M. K. P. TAYLOR, J. H. WHITELAW, AND M. YIANNESKIS, "Measurements of Laminar and Turbulent Flow in a Curved Duct with Thin Inlet Boundary Layers," NASA CR-3367, 1981.